



## Imaging and quantifying drug delivery in skin – Part 1: Autoradiography and mass spectrometry imaging

Sébastien Grégoire<sup>a,\*</sup>, Gustavo S. Luengo<sup>a</sup>, Philippe Hallegot<sup>a</sup>, Ana-Maria Pena<sup>a</sup>, Xueqin Chen<sup>a</sup>, Thomas Bornschlögl<sup>a</sup>, Kin F. Chan<sup>b</sup>, Isaac Pence<sup>c</sup>, Peyman Obeidy<sup>c</sup>, Amin Feizpour<sup>c</sup>, Sinyoung Jeong<sup>c</sup>, Conor L. Evans<sup>c,\*</sup>

<sup>a</sup> L'Oréal Research and Innovation, 1 avenue Eugène Schueller BP22, 93600 Aulnay-sous-Bois, France

<sup>b</sup> Simpson Interventions Inc., Woodside, CA 94062, United States of America

<sup>c</sup> Wellman Center for Photomedicine, Massachusetts General Hospital, Harvard Medical School, CNY149-3, 13th St, Charlestown, MA 02129, United States of America

### ARTICLE INFO

#### Article history:

Received 12 August 2019

Received in revised form 21 October 2019

Accepted 18 November 2019

Available online 26 November 2019

#### Keywords:

Human skin  
Drug delivery  
Imaging  
Autoradiography  
MALDI  
Static SIMS  
Dynamic SIMS

### ABSTRACT

In this two-part review we present an up-to-date description of different imaging methods available to map the localization of drugs on skin as a complement of established *ex-vivo* absorption studies. This first part deals with invasive methods which are grouped in two classes according to their underlying principles: i) methods using radioactivity such as autoradiography and ii) mass spectrometry methods such as MALDI and SIMS. For each method, a description of the principle is given along with example applications of imaging and quantifying drug delivery in human skin. Thanks to these techniques a better assessment of the fate of drugs is obtained: its localization on a particular skin structure, its potential accumulation, etc. A critical comparison in terms of capabilities, sensitivity and practical applicability is included that will help the reader to select the most appropriate technique depending on the particular problem to be solved.

© 2019 Elsevier B.V. All rights reserved.

### Contents

1. Introduction . . . . .	137
2. Autoradiography . . . . .	138
3. Methods using mass spectrometry . . . . .	139
3.1. Matrix assisted laser desorption ionization mass spectrometry . . . . .	140
3.2. Static secondary ion mass spectrometry . . . . .	141
3.3. Dynamic SIMS and NanoSIMS . . . . .	143
4. Methods comparison . . . . .	144
5. Conclusion . . . . .	145
References . . . . .	145

### 1. Introduction

Covering most of the surface of the body, the human skin is a major route of exposure to a wide range of compounds, spanning from drugs and cosmetics to environmental hazards. The uptake of compounds

into the skin can be desirable as in the case of topically applied drugs developed by the pharmaceutical industry. Topical drugs can be applied directly where is needed avoiding potential systemic side effects [1], as well as providing the means for sustained drug release. In the case of cosmetic products, skin is the exclusive exposure route. Besides these controlled uses, there are concerns regarding the uptake of chemicals into the skin in occupational and accidental scenarios, such as exposure to agrochemicals for farmers, or exposure to hair dyes for

\* Corresponding author.

E-mail addresses: [sebastien.gregoire@rd.loreal.com](mailto:sebastien.gregoire@rd.loreal.com) (S. Grégoire), [evans.conor@mgh.harvard.edu](mailto:evans.conor@mgh.harvard.edu) (C.L. Evans).

hairdressers. Each of these scenarios require detailed skin absorption information.

Understanding the spatial and temporal distributions of pharmaceutical compounds in target tissues and organs has become increasingly important during drug development. In dermatology, understanding the rules describing the delivery of drugs applied topically is required. It concerns the ability of a chemical to pass through different pathways, mainly through the skin barrier (e.g. *stratum corneum* (SC)) or through the hair follicle. Such information is mandatory in early stages of drug development, since active pharmaceutical ingredients are screened in order to optimize drug selection, drug concentration and formula. The distribution of active pharmaceutical ingredient (API) in the skin over time provides useful information to address safety issues and efficacy before initiation of a clinical study. For example, the SC accumulation of an API exhibiting a slow epidermal and dermal diffusion could be related to poor aqueous solubility and thus limit its bioavailability. On the contrary, it could be a cause of adverse effects, such as irritation. Local side effects such as skin irritation or skin sensitization are sufficient reasons to stop API development, even if the ingredient reaches the target tissues. In such a case alternative APIs can be developed. Imaging methods capable of quantifying drug uptake can guide clinical research and may predict clinical outcome before significant investment is made to conduct large and/or long-term clinical studies. In the cosmetics industry, skin absorption studies are crucial for skin [2] and systemic [3] safety assessments. Refining absorption estimation has become a major concern since animal testing, used to support the marketing of cosmetic ingredients, has been banned within the EU.

For topically-applied drugs, cutaneous bioavailability is also a critical parameter. Many factors affect the ability of a drug to pass into and through the skin. The level of cutaneous absorption can vary up to a factor of 80, depending on the exposed body surface area [4] and the applied compound. External factors such as UV exposure can also affect skin absorption with contrasting effects [5]. Whereas percutaneous absorption on *ex vivo* human skin of lipophilic compounds, such as octocrylene, increased after UV exposure, hydrophilic compounds such as caffeine were not affected. For nanoparticles, depending on the model used, data can be contradictory. Skin penetration of quantum dot nanoparticles increased *in vivo* in mice after ultra violet (UV) irradiation [6], but in *ex vivo* human skin, penetration of nanosized titanium dioxide is not affected by UV exposure [7]. Barrier function can be also physically disturbed [8] through, for example, tape stripping, abrasion, delipidization with solvents or treatment with sodium lauryl sulfate, [9]. While such approaches have been used to mimic percutaneous absorption through diseased skin [10], comprehensive studies of drug and compound uptake are lacking. Interestingly, a limited number of *in vivo* studies on diseased skin (e.g. atopic dermatitis, psoriasis) have shown modest increase in penetration compared to normal skin [10].

Practically, current skin absorption studies are usually performed on *ex vivo* skin. Guidelines do exist that define clear criteria to conduct skin absorption studies [11]. Such guidelines point to *ex vivo* human skin as the gold standard, with porcine skin often available as an alternative [12]. Moreover, these guidelines define clear criteria on the skin quality. Indeed, inappropriate handling may result in damage of the SC, hence the integrity of the prepared skin must be checked [13].

*Ex vivo* human skin does not describe all aspects of the *in vivo* situation. For example, the microbiome and vascular network are not taken into account with *ex vivo* skin. While *ex vivo* studies allow the measurement of the drug amount within the different skin layers (i.e. SC, living epidermis, dermis), they do not provide information on the precise spatiotemporal flow and flux of drugs within these layers or otherwise the effects of perfusion on the drug pharmacokinetics. For example, current tools do not determine the drug amount specifically residing in the hair follicle, nor measure the outward flux of compounds from the sebaceous gland into the surrounding tissue and blood vessels. This missing localization information could inform on the key diffusion pathways of compounds in the skin such as inter-cellular, trans-cellular,

appendages-to-tissue (hair follicle, sweat duct) flow [14], and systemic delivery. While this data can be directly used to determine pharmacokinetic parameters, they can also be gathered with the goal of developing simulation methods for topical exposure determination [15].

To overcome these limitations, an evaluation with appropriate imaging methods is needed. Indeed, drug imaging methods offer the ability to address and overcome the limitations of classical skin absorption studies both *ex vivo* and *in vivo* for the direct assessment of the uptake of compounds in living skin. The available imaging toolbox spans spatial and temporal resolutions, specificities, sensitivities, and offers capabilities that can be qualitative or quantitative, invasive or non-invasive, and destructive or non-destructive in nature. Each method has its own limitations and advantages. The appropriate methods being chosen according to the question, the compound itself, and the properties to be measured [16].

Imaging methods can be separated into two groups, with the main divider being the invasive and destructive nature of the approach. This first part of our review article is focused on invasive methods and aims at providing an up-to-date review of the available imaging methods for human skin compound delivery studies. They are grouped in two classes according to their underlying principles: i) methods using radioactivity such as autoradiography; ii) mass spectrometry methods including Matrix Assisted Laser Desorption/Ionization (MALDI), Static and Dynamic Secondary Ion Mass Spectrometry (SIMS). Each imaging method will be described according to the previously listed criteria and application examples in human skin drug delivery studies will be provided. The second part of our review article will be focused on non-invasive, non-destructive imaging methods that can be applied *in vivo*: i) fluorescence (conventional, confocal and multiphoton) and harmonic generation microscopies and ii) vibrational spectroscopic imaging methods (infrared and confocal Raman microspectroscopies, coherent Raman scattering microscopy and other vibrational techniques). We will also provide the reader with a decision tree flow chart of imaging methods available for human skin *ex vivo* and *in vivo* drug delivery studies.

## 2. Autoradiography

Radioisotopes have been widely used for skin absorption studies and are still recognized as a gold standard [11] despite recent papers showing good agreement between radiolabeling and classical chromatographic analysis [17]. While radiolabeling provides information on the amount of compounds which move across the skin, it yields no information on the penetration route or on the localization of the penetrant within the skin. To overcome this issue, autoradiography can be used. The particles emitted by the radioisotope label, such as beta particles, interact with photographic emulsions to provide an image. The technique itself is over 100 years old, but has been applied to skin absorption for 60 years. In 1956, distribution of hydrocortisone in human skin after topical application was evaluated on the upper back of human volunteers under occlusive conditions [18]. Biopsies were taken over the course of 1 to 16 h after application, with the radioactive material found in the epidermis after one hour but disappeared entirely from the skin after sixteen hours. Such studies are informative, but excessively invasive: 5 biopsies on each volunteer were done for the first part of the study. Over the years, autoradiography was used *in vivo* on different species and different type of chemicals (germicides on Guinea pig [19], oils on rabbit [20]). It allowed their localization in specific skin areas (i.e. epidermis, appendages, papillary dermis, reticular dermis) [21]. In the 90's, the performance of autoradiography for skin imaging was improved to a subcellular level with high sensitivity [22]. Only 30 pmol  $^3\text{H}$  estradiol per  $\text{cm}^2$  dissolved in Dimethyl Sulfoxide was necessary to be detected in various areas of rat skin (i.e. epidermis, sebaceous gland, dermal papillae of hair and fibroblasts). Micro-radiography (MARG) was used with different chemicals to assess trans-follicular delivery [23]. An aqueous gel containing radiolabeled

linoleic acid was applied on fresh human scalp obtained after plastic surgery. The combination of classical skin distribution studies and micro-autoradiography demonstrated the preferred trans-follicular pathway of linoleic acid.

Stumpf et al. [24] used MARG to localize different drugs topically applied *in vivo* on rat skin. Thin 4  $\mu\text{m}$  thick sections were used because thicker sections lead to chemical and mechanical artifacts. Before the sections were exposed to nuclear emulsions, they had to be dried in a lightproof dessicator within a freezer. The drying duration depends on concentration in the tissue and is determined empirically. Such a step could last as long as eight months [25]. Fig. 1 reported autoradiograms obtained from  $^3\text{H}$  labelled  $^3\text{H}$ -estradiol (a-c) and  $^3\text{H}$ -1,25(OH) $_2$ Vitamin D $_3$  (d). Each black dot was associated with a labelled chemical. The two classical routes of penetration were clearly observed: trans-epidermal and trans-follicular (Fig. 1a and b). The strong signal in upper layer of

the skin (*i.e.* SC) demonstrated retention in the SC and slow release deeper into the skin (Fig. 1c). Fig. 1d was obtained with labelled hormone (*i.e.*  $^3\text{H}$ -1,25(OH) $_2$ Vitamin D $_3$ ) at higher resolution (*i.e.* cellular-subcellular). At such resolution, the chemical was localized in cells of the *stratum granulosum* (small arrow) and specifically in the cytoplasm of *stratum spinosum* and *stratum basale* (large arrow).

MARG has some limitations [26] beyond the challenges involved in radiolabeling. In particular, the method only detects the presence of the radiolabel, and is not specific nor related to specific chemical structures. This presents major challenges in skin, which displays well-known metabolic activity that acts to alter topically-applied chemicals over a range of timescales [27]. For example, in the case of the topically applied molecule vaniline, cutaneous metabolism reduces the concentration of the parent compound to only 0.6% of the total amount found in receptor fluid. Thus, MARG misses the metabolic information of the overall absorption, distribution, metabolism, and excretion (ADME) process. A related problem can also be found when studying chemicals having low levels of absorption, as uncertainty in the radiographic measurement can arise due to the presence of radiolabeled impurities. To overcome this issue, analysis should be completed with radio-HPLC coupled with mass spectrometry [28]. The other main concern with MARG is the challenge in obtaining robust quantitative information [29], as radiographic studies can have numerous artifacts that must be understood and controlled to achieve quantification.

These radiographic techniques can be informative in understanding drug and compound uptake, in particular when samples can be prepared as thin radiolabeled histological sections. Autoradiography offers information on drug localization (epidermal and dermal layers, appendages, etc.) and penetration pathways with subcellular resolution. However, this approach can be time consuming and, on its own, lacks metabolic and chemically-specific quantitative information.

### 3. Methods using mass spectrometry

Alternative methods to autoradiography have been developed that largely eliminate the need for radiolabeling and provide specific chemical information [26]. Mass spectrometry is one of the methods dedicated for such tissue imaging. Mass Spectrometry Imaging (MSI) has several advantages [30] that make it an attractive tool for studying the uptake of compounds into skin. MSI tools provide structural information, as the acquired data is related to the molecular weight of the detected species. Thus, MSI allows detection of chemicals and their metabolites [31] with spatial resolutions on the cellular to subcellular scale. Moreover, MSI methods have the capability to image thousands of molecules such as xenobiotics, metabolites, lipids, peptides, and related compounds, providing a large picture of the local chemical environment. Importantly, these methods do not require specific labelling, and are therefore applicable to a far greater range of compounds than radiographic approaches.

Whatever the mass spectrometry method, the principle is fundamentally the same [32]: thin slices are prepared and the tissue is flash-frozen. Other sample preparations, such as formalin fixation, are challenging but not incompatible with MSI. Indeed, most chemicals react through cross linking and thus interfere with ionization. Moreover, several classes of endogenous molecules (*i.e.* lipids) and some API can be washed or delocalized by the fixation or dewaxing steps. It can therefore lead to some misinterpretations and false positive/negative results. However several groups have described the use of MSI on this type of tissues [33]. The sample is then placed into the MSI device and mapped. The mass spectrometer scans the beam across the sample, ionizing the molecules on the surface of the sample. Ions are then transferred to an analyzer to measure their mass-to-charge ( $m/z$ ) ratios, resulting in a mass spectrum collected at each pixel on the tissue section. Using computational software, the mass spectrum at each point on the sample can be used to compute an ion density map, generating a visual distribution of the different components within the sample.

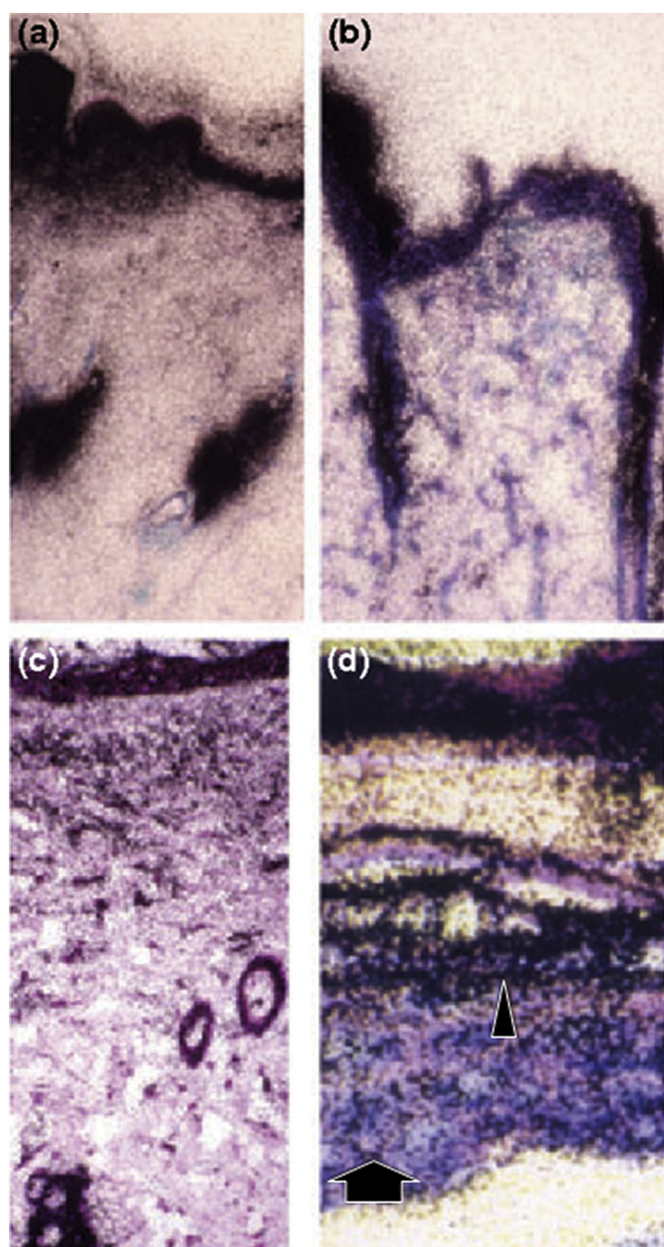


**Fig. 1.**  $^3\text{H}$ -oestradiol (a-c) and  $^3\text{H}$ -1,25(OH) $_2$ vitamin D $_3$  (d) were topically applied *in vitro* on rat skin. At high resolution, autoradiogram of vitamin derivate (d) shows accumulation in interstitial material of *stratum granulosum* (small arrow) as well as accumulation in cytoplasm cells of *stratum spinosum* and *stratum basale* (large arrow). Copyright (2019), with permission from John Wiley and Sons [25].

Intrinsically, mass spectrometry is highly specific as the measurement is associated with discrete mass values. This specificity can be further increased using high resolution mass spectrometry methods such as Time of Flight (TOF), Fourier Transform-Ion Cyclotron Resonance (FT-ICR) or Orbitrap™ configurations. Many different ionization modes have been developed for MSI, with the most commonly approaches being Desorption Electrospray Ionization (DESI) [34], Matrix Assisted Laser Desorption Ionization (MALDI), Static Secondary Ion Mass Spectrometry (SIMS), and Dynamic SIMS. Of these four methods, DESI is the only one effective at ambient pressure, however its resolution is low [35,36] at typically several hundred microns laterally. This makes DESI poorly suited for localizing chemicals in specific structures within skin. In the following, we will describe the principles and applications of the remaining mass spectrometry ionization methods in human skin drug delivery studies.

### 3.1. Matrix assisted laser desorption ionization mass spectrometry

At the end of the 1980's, Karas and Hillenkamp [37] developed MALDI as a new ionization method. Less than ten years later, the first application of MALDI for tissue imaging was carried out on rat pancreas tissue, rat pituitary tissue, and human mucosa cells [38], with the first application of MALDI imaging to skin tissue carried out a few years later [39].

MALDI operates by distributing a matrix having ultraviolet absorption properties homogeneously on a thin histological skin section. The sample is then irradiated with an UV pulsed laser that promotes the ionization of the matrix and the desorption of the chemical. In the formed plasma, the chemical is ionized through proton transfer from ionized matrix species. The nature of the matrix has to be chosen according to the chemical being analyzed [40]. For tissue imaging, other critical points have to be taken into account to ensure high quality images. The first key point is related to the tissue preparation [40]. Thin histological sections with a thickness between 10 and 20  $\mu\text{m}$  are typically prepared using a cryomicrotome, with the optimal tissue thickness being approximately 12  $\mu\text{m}$  [41]. While such slices are obtained from frozen samples, new embedding approaches have been proposed to overcome limitations of the flash-freezing process [40]. The second key point for sample preparation is related to matrix deposition [42]. This process should be carefully controlled to properly define the crystal matrix size [40]. Different approaches have been proposed, with the most commonly used method being pneumatic nebulization [40].

Mass spectrometry coupled to a liquid chromatographic system (LC/MS) is currently the most common technique for quantitative bioanalysis [43], making it a gold standard for comparison to MALDI approaches. Many studies claim that MALDI can offer absolute quantitative results similar to those achieved *via* LC/MS [26,40]. A common issue for quantification with mass spectrometry and particularly with electrospray is the matrix effect. When a chemical of interest is ionized, other chemicals coming from the samples could be ionized too. A competition could take place between the different components affecting the ionization efficacy of the chemical of interest. Variation of the signal according to the sample analyzed is name matrix effect. It is not related to the matrix used in MALDI. This same competition is effective in MALDI. For example, when the laser irradiates a sebaceous gland the composition of the tissue is different from another area such as epidermis. Thus the ionization efficacy could be different from area to area. To overcome this issue, an internal standard is used [43]. This standard is chosen to mimic the behavior of the chemical during the ionization process; a stable, labelled version of the analyte is the most appropriate, followed by a structurally similar compound as a secondary choice. The tissue section is coated with the internal standard [31]. If the internal standard is lacking, Hamm et al. [44] proposed to use a normalization factor called TEC (Tissue Extinction Coefficient). MSI quantification *via* MALDI has been demonstrated through a multicenter validation study [45]. Precision and accuracy of the clozapine MSI

quantification was measured on isolated perfused rat liver and compared with classical LC/MS quantification. The study showed that MSI quantification accuracy was approximately 80% of the value obtained by LC/MS on an adjacent tissue section.

The resolution of this imaging method is also a key point. Some skin compartments are very thin (*i.e.*  $\sim 10\ \mu\text{m}$  for the SC [46]), making it important for an imaging method to reach single micrometers of resolution. The resolution achievable with MALDI depends on the diameter of the laser spot, and more precisely the effective excitation or ablation area. For most studies, the resolution of MALDI has been between 25 and 100  $\mu\text{m}$  [31,47], and can go up to 200  $\mu\text{m}$  [39]. Importantly, higher resolutions have been demonstrated, with pixel sizes of 500 nm and a resolving power of 4  $\mu\text{m}$  [48].

The first example of MALDI imaging of compounds within the skin was carried out on pig skin treated topically with a ketoconazole shampoo [39]. MALDI has also been used to map lipids in *ex vivo* human skin [49]. By lowering the resolution from 150 to 30  $\mu\text{m}$ , different substructures were identified, such as the epidermis or adipocytes within the hypodermis. The epidermal growth factor receptor-tyrosine kinase inhibitor erlotinib was visualized using MALDI in rat and human skin after oral exposure [50]. Localization of erlotinib in the superficial skin layer has been associated with rashes, making this finding important. Other examples have been reported in a recent review [51]. However, none of these examples demonstrate the performance of MALDI imaging for chemical localization in the substructures of the skin.

Few examples are available to demonstrate that MALDI imaging can be used to investigate the capability of a chemical to reach the sebaceous gland after topical exposure. Hunt et al. [52] evaluated Olumacostat Glasaretil, a small molecule inhibitor of acetyl coenzyme A carboxylase, either on hamster ear skin or pig ear skin. MALDI imaging was used to confirm specific drug distribution in the sebaceous gland. Another example was obtained with a formulation containing nobiletin (CAS Number 478-01-3, Sigma Aldrich, Lyon, France) at 1% applied at 5 mg/cm<sup>2</sup> on pig inner ear skin for 16 h. This model was ideal for investigating drug uptake *via* the hair follicle pathway [53], and thus appropriate for sebaceous gland targeting. The skin surface was washed with a cotton swab soaked with isopropanol/water (20/80 v/v), and a gentle massage was performed for 30 s prior to freezing at  $-80\ ^\circ\text{C}$  in isopentane. The study was performed on one donor in duplicate and one sample from the same donor was also treated with a placebo. Twelve nobiletin-treated consecutive sections and four placebo-treated consecutive sections at 10  $\mu\text{m}$  thickness were collected. Over two consecutive sections, one section was used for H&E staining and the other one for MALDI imaging.

The sections were placed on Superfrost slides for imaging and dried at room temperature. A matrix solution of 6-aza-2-thiothymine solubilized at 10 mg/ml in a mixture 50/50 v/v (acetonitrile/water + 0.1% (v/v) trifluoroacetic acid) was sprayed onto the slides with an automatic sprayer (SunCollect, Sunchrome, Friedrichsdorf, Germany). Analyses were performed by direct analysis with a 7 T-MALDI-FTICR in positive CASI mode using 50  $\mu\text{m}$  spatial resolution. All images were acquired by Imabiotech (Lille, France) and analyzed with Multimaging (Imabiotech, Lille, France).  $[\text{M} + \text{H}]^+$  of Nobiletin was detected at  $m/z$  403.1387. High resolution performance of FT-ICR ( $m/\Delta m = 150,000$ ) guaranteed the specificity of signal. Ideally, a fragment ion has to be detected and used to confirm the chemical identity. Unfortunately, no fragment ion was observed in Nobiletin mass spectra. Thus, specificity was guaranteed with high resolution performance of the mass spectrometer. No signal was observed at  $m/z$  403.1387 on the placebo-treated tissues thus proving the specificity of the signal on the treated tissues. Fig. 2 shows a typical MALDI image at  $m/z$  403.1387 of a skin sample treated with a formulation containing nobiletin. The signal of the ion at  $m/z$  403.1387 was normalized to the maximum signal measured on the image. This normalized signal was converted into a color scale from 3% to 0.01%. Some specific areas showed higher signal than others. To identify the anatomical zone associated with this area, an

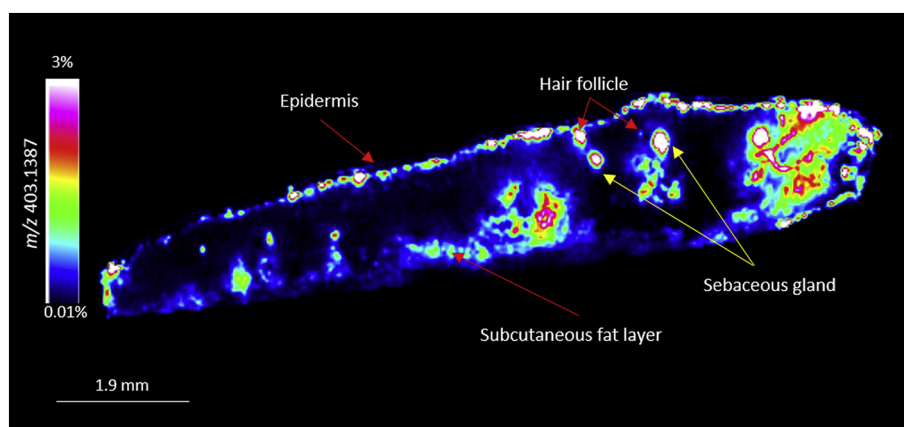


**Fig. 2.** Nobiletin molecular ion ( $m/z$  403.1387) distribution on pig inner ear skin tissue treated with formulation containing 1% Nobiletin (sample 1 replicate 3). Color scale is the intensity normalized to the maximum signal observed on the image and ranked from 3% to 0.01% of this maximum signal.

overlay with H&E staining was performed. Indeed, serial tissue sections were used for imaging and histology. Overlay between two consecutive slices (one for MALDI imaging and one for H&E staining) enabled localization of the compound within the skin (see Fig. 3). The spot observed on Fig. 2 was clearly associated with sebaceous gland.

Imaging was carried out using a spatial resolution of 50  $\mu\text{m}$ . The thin layer on the upper part of the image corresponds to SC and partially visible region of the epidermis. Given the thinness of the epidermal layer, these images show that a spatial resolution of 50  $\mu\text{m}$  does not allow clear discrimination of the SC from the epidermis. The results clearly show that nobiletin was able to reach the sebaceous gland, suggesting a trans-follicular pathway for uptake. Indeed, a significant amount of nobiletin was found in the upper part of the hair follicle surrounding the sebaceous glands. However, none of the sections allowed direct visualization of the pathway along the hair follicle.

This example demonstrated the performance of MALDI imaging as an appropriate method to target macrostructures in the skin such as sebaceous glands or hair follicles. As the example shows, the usual MALDI resolution (*i.e.* 25 to 100  $\mu\text{m}$ ) should be not great enough to visualize the localization of compounds within the epidermal layer of the skin. Mean SC thickness of pig ear skin is around  $13.13 \pm 1.8 \mu\text{m}$  and mean epidermis thickness is at  $44.63 \pm 4.26 \mu\text{m}$  [54]. Thus between 1 and 2 pixels can be obtained. Human epidermis thickness is thicker, with mean values ranking from 56.6 to 81.5  $\mu\text{m}$  depending on the anatomical site

[55]. In some specific diseases like psoriasis, the epidermis is thicker [56] by a factor 2. The number of pixels remains limited. Several papers describing the development of a MALDI ion source that can achieve a spatial resolution up to 5  $\mu\text{m}$  had been reported for proteomic [57,58], metabolomic [33] or drug delivery [59] applications. More recently, Niheaus et al. [60] adapted a transmission-mode-MALDI-2 ion source to achieve subcellular resolution in brain tissue with a pixel size of 600 nm. Other mass spectrometry imaging methods are able to achieve such high resolution.

### 3.2. Static secondary ion mass spectrometry

In 1910, J.J. Thompson studied the effect of sputtering positively charged particles onto a metallic film, allowing him to investigate the effect of different elements emitted. However, it was not until 1949 when the first SIMS dedicated to surface analysis was constructed by Herzog and Viehbock. Its application for solids was further developed by Benninghoven (1969) and extended to softer materials as polymers by Briggs and coworkers (1982). The first commercial instruments appeared around 1985. SIMS has evolved into a sensitive surface analytical technique that is well established for many industrial and research applications [61,62].

SIMS is a physical chemical technology to analyze solids. It is based on the detection of secondary ionized fragments expelled after the impact of an incident sputtering ion beam (compared to a laser source with MALDI) with energies in the range of keV [63]. These ions are constituents of the primary beam. A cascade of collisions with the atoms of the solid analyzed produces bond breaking and the emission of a diversity of types of radiation and particles depending on the nature of the sample. The emergence of cluster ion sources (*i.e.*  $\text{Au}^{3+}$ ,  $\text{Bi}^{3+}$ ) for the sputtering beam improved the efficiency of this process [64]. Secondary ions are extracted, accelerated and analyzed as a function of their mass, but only represent a fraction (10–30%) of all emitted particles. Further improvements are achieved by the use of ions beams based on Buckminster fullerene,  $\text{C}_{60}^+$  (increasing yields  $\sim 1000$  times), by the use of bigger cluster ion beams,  $\text{Ar}_{2000}$  or by, in some cases, delivering water to the surface that enhances the ionization. These efforts have helped extend the applications of the technique, for example for depth profiling analysis [65]. As all MSI techniques, SIMS is invasive and requires careful sample preparation as described above. In addition, when a particular drug is being monitored, sensitivity may be an issue if its concentration is in the micromolar range [66].

The interest in mapping low molecular weight compounds such as drugs or biomarkers in tissues has boosted the use of time-of-flight (TOF) SIMS techniques. SIMS's micron-level resolution and chemical specificity makes this approach particularly well-suited for quantifying drug uptake, and as such, there are many examples of its use. SIMS

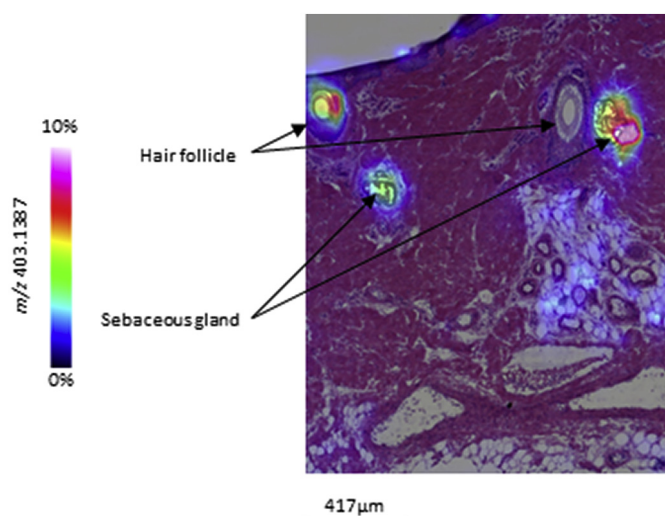


**Fig. 3.** Zoom of Fig. 2 on area of interest pointing out hair follicle and sebaceous gland. This anatomical zone is identified through overlay between Nobiletin molecular ion ( $m/z$  403.1387) MALDI imaging and H&E staining.

has been used, for example, to map and quantify cosmetics within the surface of hair [67,68]. In both hair and skin, the repartition of lipids in the fiber structure is an example of particular importance for cosmetic or dermatological applications that can be investigated *via* SIMS. This approach has enabled micrometric lipid distribution analysis in samples [69] such as in rat brain sections using  $\text{Au}^{3+}$  cluster beams [70].

The distribution of endogenous skin components and the repartitioning of molecules in a tissue section are also important to explore. This is essential not only for assessing the composition of skin, but also to study how exogenous compounds penetrate and distribute into skin tissue. The latter consideration is paramount in designing drug and cosmetic formulations. A particular drawback of SIMS is the difficulty in extracting quantitative information regarding the concentration of different species. Recent efforts addressing this limitation have shown that this challenge can be overcome when SIMS is combined with more classical Franz cell cutaneous absorption studies [71]. In these studies, TOF-SIMS was used to investigate the uptake of carvacrol (CAS number 499–75–2, Sigma Aldrich, Lyon, France) a characteristic component of essential oils. Full thickness human skin was treated for 16 h under occlusive conditions with essential oil 1% in Pemuen gel + Cyclodextrine. Then skin was frozen ( $-80\text{ }^{\circ}\text{C}$ ) in isopentane. For SIMS analysis,  $10\text{ }\mu\text{m}$  thick sections were cut using cryomicrotome, stored and measured while maintaining the same low temperature to avoid evaporation of carvacrol.

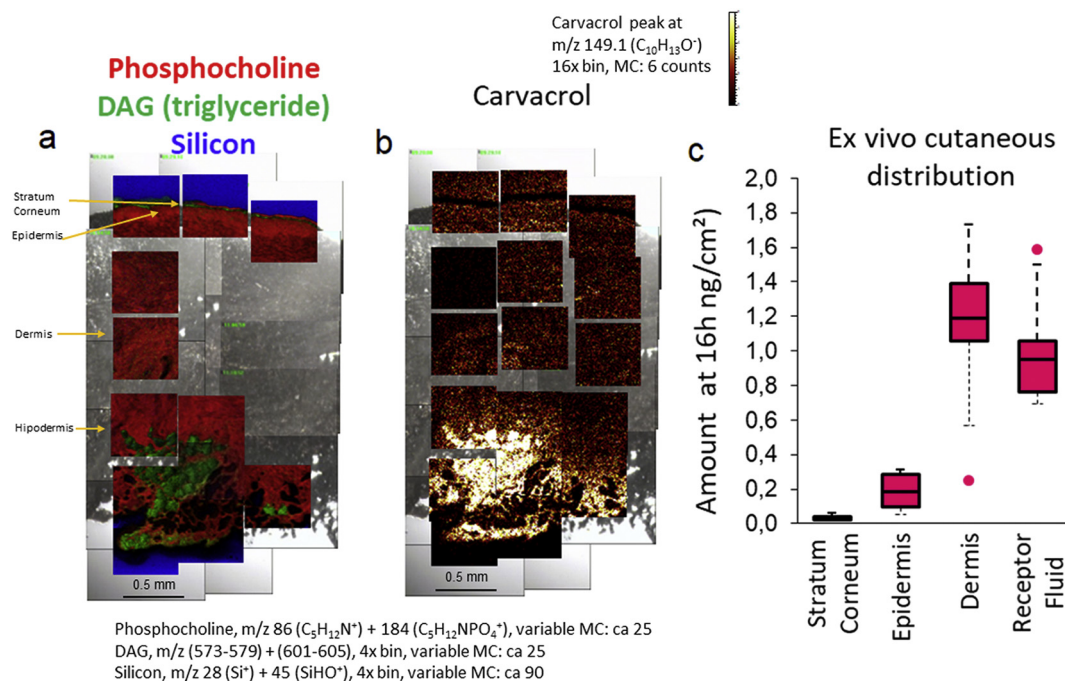
A  $\text{Bi}_3^+$  ion beam of 25 keV was used to irradiate the samples. Secondary ions were analyzed using TOF-SIMS analyzer under static SIMS conditions in a TOF-SIMS IV instrument (IONTOF GmbH, Münster, Germany). All images were acquired with SurfaceLab v6.8 (IONTOF GmbH, Germany). The positive and negative fragments were identified with the instrument either 1) tuned for low spatial, but high mass ( $m/\Delta m \approx 3000\text{--}6000$ ) resolution or 2) high spatial (lateral resolution  $\sim 500\text{ nm}$ ) and low mass ( $m/\Delta m \approx 300$ ) resolution, depending on the different regions studied.

Fig. 4a gives an example of the skin distribution of a selection of two different fragments. Phosphocholine ( $m/z\ 86 + 184$ ) comes from

endogenous phospholipids present in viable cells, and is therefore concentrated in the epidermis. Diacylglycerol (DAG) fragments ( $m/z\ (549\text{--}551) + (575\text{--}579) + (601\text{--}605)$ ) arise from typical endogenous triglycerides present either in the skin surface (sebum) or associated with adipocytes. Fig. 4b shows the distribution of the negative fragment at  $m/z\ 149.1$  corresponding to carvacrol. The small signal observed close to the surface agrees with the cutaneous distribution obtained by the classical Franz cell method (see Fig. 4c). In certain deeper skin areas, the signal was observed to be very strong. These localizations correlate to areas where DAG ions are also found, suggesting localization into adipocytes.

The detection of an exogenous ceramide R (CAS number: 54422–45–6, L'Oréal, Aulnay sous Bois, France) was also analyzed using the same procedure. The exogenous ceramide in the topical formulation was distinguished from the endogenous ceramides in the SC by their different molecular weights (endogenous 650–750 Da *versus* exogenous 565 Da). The exogenous ceramide was detected in positive ion mode at  $m/z\ 566.56, 588.53$  corresponding to  $[\text{M} + \text{H}]^+$  and  $[\text{M} + \text{Na}]^+$ , as well as in negative ion mode at  $m/z\ 564.50$  corresponding to  $[\text{M} - \text{H}]^-$ . A fragment ion at  $m/z\ 562.50$  was detected in positive ion mode corresponding either to ion fragment  $[\text{M} + \text{H} - 4\text{H}]^+$  or ion fragment  $[\text{M} + \text{Na} - \text{C}_2\text{H}_2]^+$ . The resolution of the TOF was not enough to determine the exact composition of the fragment ion. Fig. 5 indicates the localized distribution of exogenous and endogenous ceramides within the SC. Untreated skin showed no signal at  $m/z$  characteristic of endogenous ceramide either in positive or negative ion mode [71].

TOF-SIMS has also the ability to conduct depth profiling analysis as continuous sputtering of the beam penetrates the surface and reveals areas underneath. MS analysis of the fragments allows the reconstruction of 3D profiles of the sample constituents. The surface of hair can be studied in this way [72]. In the case of skin, one of the main advantages of this approach is that it can address potential problems associated with sample preparation, embedding and sectioning. Skin can be directly sputtered at the surface to slowly penetrate the different layers. Starr et al. [73] have successfully applied this method using a TOF-SIMS



**Fig. 4.** Superposition of SEM images and TOF SIMS distribution images of full thickness human skin after exposure to an essential oil compound (Carvacrol). In (a) the three color images indicate the localization of the support (silicon), phospholine and triglycerides (DAG). The images show two added  $m/z$  intervals:  $m/z\ 573\text{--}579$  and  $m/z\ 601\text{--}605$ . The first interval corresponds to DAG(34:3 + 2 + 1 + 0) and second to DAG(36:3 + 2 + 1). (b) The distribution and intensity of carvacrol is indicated. When comparing (a) and (b) the co-localisation of carvacrol and triglycerides images indicate its accumulation in fatty adipocyte areas. (c) The *ex vivo* cutaneous distribution of carvacrol using Franz cell is indicated for comparison.

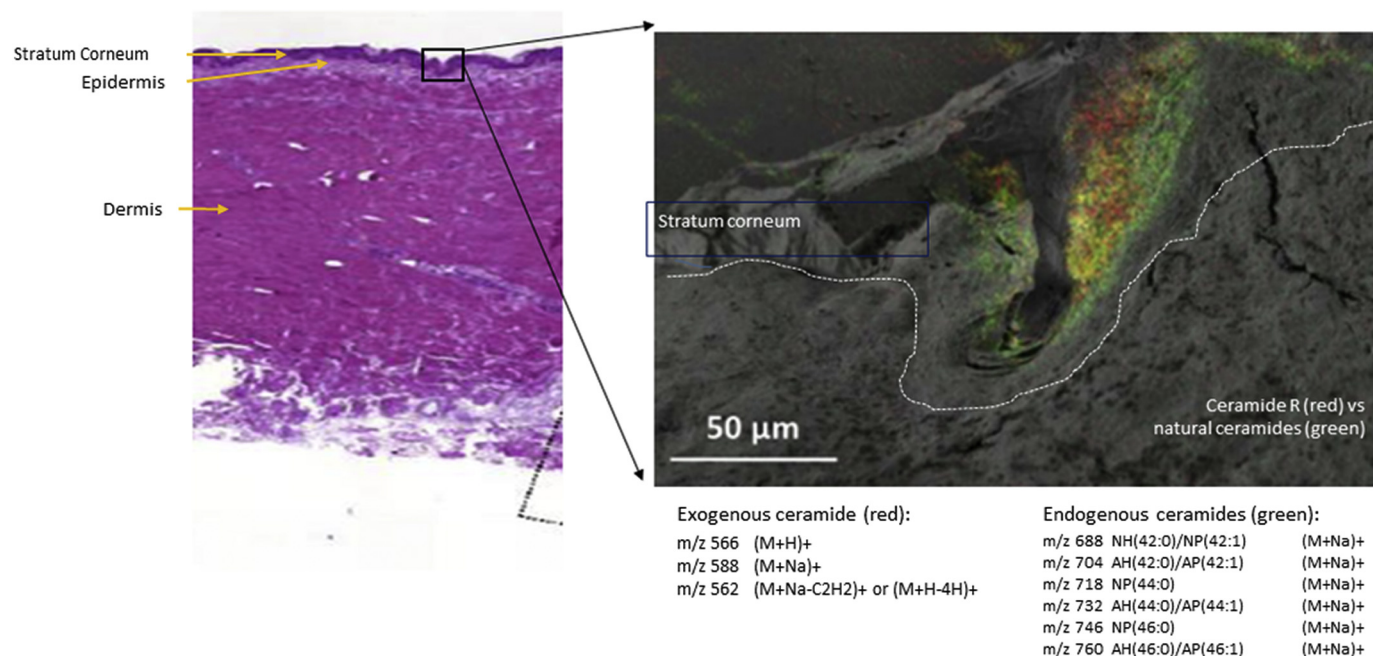


**Fig. 5.** Superposition of SEM and high resolution TOF-SIMS distribution (signal intensity) images (right) of the stratum corneum region of a skin cross histological section (left) treated with a ceramide formulation. The 2-color overlay image represent the positive ions of endogenous ceramide (m/z 688 + 704 + 718 + 732 + 746 + 760) and the exogenous ceramide (Ceramide R) corresponding to positive molecular ions (m/z 562 + 566 + 588).

IV instrument and a 25 keV Bi<sup>3+</sup> sputtering beam for the evaluation of skin permeation profiles of ascorbic acid (vitamin C) and a precursor (ascorbyl glucoside) in *ex vivo* porcine skin. An area of 500 × 500 µm<sup>2</sup> was first sputtered, while a smaller region (200 × 200 µm<sup>2</sup>) was analyzed. This study shows the potential, but also the challenges of this kind of analysis. It is critical to correctly calibrate the profiling depth as well as systematically control the sputtering rate. These considerations are especially important in mechanically non-homogeneous multilayer systems such as the skin. Accurate measurement of the final resulting crater is not sufficient to calculate a sputtering rate, as the rate itself can change depending on the resistance of the region under study. Thus, while promising, further improvements are necessary to advance this technique, either through the addition of other calibration or *via* monitoring the position and depth of endogenous components characteristic of the different skin structures. For example, phosphate-containing fragments arising from phospholipids can be used to determine when the beam has penetrated through the SC. This 3D profiling approach is a promising direction for TOF-SIMS analysis of the skin that will no doubt see further advancement in the future.

### 3.3. Dynamic SIMS and NanoSIMS

Castaing and Slodzian presented in 1962 new possibilities for isotopic imaging based on dynamic secondary ion emission [74]. The advantages of these techniques over both autoradiography and X-ray emission imaging were investigated by Galle, who went on to develop several biological applications [75–78]. The dynamic SIMS instrumentation has long been dominated by CAMERA Instruments, which have held a near monopoly going back to the first SMI 300 ion microscope [79]. Several dedicated instruments have been produced, with the NanoSIMS series taking advantage of parallel mass detection [80].

For static SIMS, primary ion levels of <math>10^{13}</math> ions per cm<sup>2</sup> are typical [81], while in contrast primary bombardment can reach levels of 10<sup>16</sup> ions per cm<sup>2</sup> in dynamic SIMS. This rather high brightness induces the fragmentation of molecules into their atomic components. As a consequence, dynamic SIMS does not in most cases give access to molecular distributions, unless the molecule of interest contains isotopes which are not present or abundant in the surrounding matrix. When a

characteristic isotope is not naturally present in the molecule, labelling can be performed to provide molecular specificity. In SIMS analysis, a wide variety of isotopes can be used for organic molecule labelling. Good candidates atoms include deuterium (<sup>2</sup>H), <sup>15</sup>N, <sup>13</sup>C, and <sup>18</sup>O, which all have a low natural abundance and a high secondary emission yield under primary bombardment.

In a NanoSIMS system, focused ion beams for negative (Cs<sup>+</sup>) or positive (O<sup>-</sup>) ion detection and imaging are scanned onto the sample surface which is consequently sputter-eroded. The eroded material is collected, and mass selected to obtain isotope distribution maps of constitutive elements of the sample. Spatial resolutions in the range of 50 nm and sensitivity down to the part per billion (ppb) have been obtained, in great part due to the high transmission efficiency of the instrument (60% at m/Δm = 5000). When simultaneous acquisition of different masses is achieved, accurate high-resolution quantitative imaging of isotope ratios can be collected. However, matrix effects involved in secondary emission preclude direct *in situ* quantitation [82].

The major requirement for NanoSIMS sample analysis is the presence of a flat surface that can withstand high vacuum. In most cases, this requires cutting or resurfacing the material after embedding, but this manipulation can displace diffusible elements or molecules of interest. Cryo-methods can help in preventing such redistribution, but because NanoSIMS systems are not equipped with a cryostage, cryosections or resurfaced frozen samples cannot be directly analyzed. To circumvent this limitation, Burns and File developed a sample preparation technique consisting in fast freezing, lyophilizing, and embedding samples in Spurr resin [83]. After curing, the resin block can be cut or resurfaced at room temperature and sections or the block subsequently introduced in the NanoSIMS chamber for analysis. This sample preparation technique has been much improved by careful control of the freeze-drying process at 0.2 Pa from -110 °C to -10 °C in about 8 days, followed by Spurr's resin infiltration from -10 °C to 20 °C, the epoxy resin being then polymerized at 65 °C [84]. Freeze-drying and resin-embedding method has been successfully applied to image highly diffusible element distributions from surfaced blocks of human hair shaft [85]. These efforts and others have led to dynamic SIMS instruments with high spatial resolution (UC-SIM) [86] and NanoSIMS has found many applications in biology [87–90].

Although dynamic SIMS in a NanoSIMS appears to be extremely promising for the investigation of drug delivery pathways in skin, few papers can be found in scientific literature on this subject. Skin related studies based on NanoSIMS isotope imaging are mainly driven by the Research Center of the Curie Institut, Orsay F-91405, in Guerquin-Kern's laboratory. In fact, NanoSIMS has been an invaluable tool for the target identification of isotopically labelled antitumoral drugs for melanoma treatment [91–93]. However, NanoSIMS has also been used for more conventional studies of molecule penetration in SC, where the high spatial resolution of the instrument provided access to the intercellular network of the uppermost layers of the epidermis for cosmetics evaluation [94].

A new promising SIMS technique has recently emerged with the advent of the npSCOPE that seeks to push the analytical limit of SIMS imaging down to a theoretical 10 nm spatial resolution [95].

#### 4. Methods comparison

The imaging methods described above all have a common limitation: they require thin tissue sections prepared from *ex vivo* skin biopsies. Such methods can be compared according to different criteria. Table 1 summarizes the performance of each method in skin drug delivery studies according to some criteria such as spatial resolution, sensitivity and the extracted semi- or quantitative information.

Each method has its own advantages and disadvantages. MARG is a powerful method with great sensitivity related to both labelling and subcellular resolution. Moreover, performance of MARG requires well controlled conditions and can take from days to weeks or even months to reach optimal results in terms of spatial resolution and quantification [26]. However, this method requires sample labelling with radioisotopes such as Tritium or  $^{14}\text{C}$ . Specificity of the method depends on the purity of the radiolabelled chemical. Actually, since no chemical identification is performed, any labelled impurities can contribute to the measured signal. Moreover, if chemical is metabolized, metabolites cannot be identified. NanoSIMS displays the same limitations, particularly if labelling with stable isotopes is used. MSI tools, such as MALDI and static SIMS are attractive alternatives. The specificity of these methods are mainly related to the performance of the resolving power of the mass spectrometer. For such purposes, a High Resolution Mass Spectrometer (HRMS) has to be used to guarantee analytical specificity. All HRMS do not have same resolving power: FT-ICR and Orbitrap™ have better resolving power than TOF and thus specificity with FT-ICR and Orbitrap™ are better. Moreover, mass spectrometry can provide molecular information through  $m/z$  measurements of the detected ions. Thus, drugs and their metabolites can be uniquely identified [31].

Methods can be separated into quantitative methods (MARG, MALDI) and semi-quantitative methods (SIMS, nanoSIMS). Quantitative method performance is characterized by different factors including dynamic range of quantification. MARG can display a large dynamic range covering up to 4 orders of magnitude [29]. The typical dynamic range of MALDI-TOF experiment was 2 log of concentration [44]. This dynamic range remained limited to 2 orders of magnitudes even when using more recent TOF instrument [96], using a linear ion trap mass spectrometer [97], or with FT-ICR (used for Nobiletin study described previously).

Sensitivity of the method is another major criteria of comparison. The ability of an analytical method to detect the lowest amount of chemical in a given sample defines its limit of detection (LOD). For such imaging methods, LOD can be expressed in  $\mu\text{g/g}$  ( $\mu\text{g}$  equivalent drug /g of tissue).

Considering the definition of LOD (e.g.  $S/N > 3$ ) [98], the absolute limit of detection can be evaluated with radioactivity. Using the calculation defined by Solon [29] and considering usual specific activity (i.e. 50 mCi/mmol), LOD is estimated around 0.6 ng/g for a chemical with a molecular weight at 300 Da. Using Quantitative Whole Body Autoradiography (QWBA), LOD was measured at 7 ng/g for Finerone in a male rat 1 h after oral administration of 3 mg/kg [99]. Using same method, LOD was measured at 118 ng/g for small peptides in rat 12 h after IV administration.

Schulz et al. [100] recently reviewed applications of MALDI imaging in pharmaceutical research and drug development. In the same study with laser beam at 20  $\mu\text{m}$ , Hamm et al. [44] evaluated two different chemicals: Propranolol and Olanzapine. Propranolol was 50 more sensitive than Olanzapine, with LOD at 0.077 and 4.7  $\mu\text{g/g}$ . On mice tumors at a lower spatial resolution (i.e. 100  $\mu\text{m}$ ), LOD of Rifampicine was measured at 0.2  $\mu\text{g/g}$  [101]. LOD for Nobiletin on pig skin, previously described, with a resolution at 50  $\mu\text{m}$  was at 4.3  $\mu\text{g/g}$ .

For static SIMS, Lockyer [102] reported a LOD in the  $\mu\text{g/g}$  range. For the study done with Carvacrol [71], the LOD could be estimated above 71  $\mu\text{g/g}$ . Indeed, in Fig. 3 no significant signal was measured in SC. Considering the mean amount measured in SC at 71 ng/cm<sup>2</sup> and a mean thickness of SC, the mean concentration in SC was at 71  $\mu\text{g/g}$ . As the TOF-SIMS method was not able to detect Carvacrol in SC, the limit of detection should be above this mean concentration. CAMECA is the developer and supplier of the NanoSIMS. They measured sensitivity for dynamicSIMS at its ultimate spatial resolution to be 100  $\mu\text{g/g}$  for 50\*50\*10 nm pixel. The ability to image the spatial distribution of a molecule in a biological tissue will greatly depends of the secondary emission yield of the isotope used as a label, of the number of labels attached to the molecule, and of the natural abundance of the label in the biological matrix. With a suitable emission yield, a convenient substitution with HYDROGEN, and a very low natural abundance, DEUTERIUM is often a good candidate.

Despite no common chemicals to compare these different methods, All these data allow to rank method according to their sensitivity. MARG is the most sensitive method, and MALDI is more sensitive than static SIMS. Dynamic SIMS is the least sensitive method.

When imaging methods are compared, one of the key criteria is the spatial resolution. As pointed out previously, each method has been optimized. Greatest spatial resolution is obtained with nanoSIMS with a usual resolution at 50 nm and with ultimate performance at 10 nm [95]. MARG could reach a subcellular resolution around 100 nm [25]. StaticSIMS can achieve a usual resolution at 2  $\mu\text{m}$ . This resolution can be further improved to 500 nm [71]. MALDI had the lowest resolution, usually between 25 and 100  $\mu\text{m}$ . Some recent results have shown ultimate resolution at 600 nm [60]. According to the spatial resolution, the methods can be ranked follows: MARG > NanoSIMS > SIMS > MALDI.

**Table 1**  
Comparison of imaging methods regarding the spatial resolution, sensitivity, quantification and dynamic range.

	Chemical	Spatial resolution	Sensitivity	Semi- / Quantitative	Dynamic range
Dynamic SIMS	Labelling with stable isotopes (D, $^{13}\text{C}$ , ...)	50 nm (max 10 nm [95])	$\approx 100 \mu\text{g/g}$	Semi quantitative	NA
Static SIMS	Ionisable with SIMS	2 $\mu\text{m}$ (max 500 nm [71])	$\approx 1 \mu\text{g/g}$ [102] Carvacrol: 71 $\mu\text{g/g}$ [71]	Semi quantitative	NA
MALDI	Ionisable with MALDI	25–100 $\mu\text{m}$ (max 600 nm [60])	Propranolol: 0.077 $\mu\text{g/g}$ [44] Rifampicine: 0.2 $\mu\text{g/g}$ [101] Nobiletin: 4.3 $\mu\text{g/g}$ Olanzapine: 4.7 $\mu\text{g/g}$ [44]	Quantitative	2 order of magnitude
MARG	Labelling with radioactive isotopes ( $^3\text{H}$ , $^{14}\text{C}$ , ...)	100 nm	Theoretical: 0.6 ng/g [29] Finerone: 7 ng/g [99]	Quantitative	4 order of magnitude

Several questions must always be addressed when selecting the most appropriate imaging methods for human skin drug delivery studies. Can the chemical be radiolabeled? Is quantitative information needed? What do we target in skin? Should the metabolite be identified? However, the most fundamental question that precedes all these is: can excised skin be obtained? If the answer is no, none of the invasive methods described here are appropriate.

## 5. Conclusion

For topically delivered drugs, cosmetics applied on the skin, or pesticides with occupational topical exposure, cutaneous absorption is usually assessed through *ex vivo* skin studies. Such assays are useful for risk assessment, but they lack information on the route of penetration or the targeting of specific skin sub-layers.

In this first part of our review, we described several invasive imaging methods offering the ability to address and overcome these limitations in *ex vivo* human skin drug delivery studies. However, no method is ideal: the advantage of one method is often being a disadvantage of another one. For example, Static SIMS has a greater spatial resolution than MALDI, however, MALDI can provide quantitative information. Moreover, some chemicals cannot be easily labelled either with stable or radioactive isotopes. If such chemicals are not easily ionized with MALDI or SIMS, none of these invasive imaging methods can be used. In this case, other imaging methods need to be developed and employed depending on the optical properties of the chemical to be characterized.

The optical imaging methods, described in more details in the second part of our review, are grouped in two classes: i) fluorescence (conventional, confocal and multiphoton) and harmonic generation microscopies and ii) vibrational spectroscopic imaging methods (infrared, confocal Raman microspectroscopies, and coherent Raman scattering microscopy). Their non-invasive character, sub-cellular resolution, and specificity hold promise for spatiotemporal quantification of compounds within *in vivo* human skin.

## References

- [1] S. Wiedersberg, R.H. Guy, Transdermal drug delivery: 30+ years of war and still fighting! *J. Control. Release* 190 (2014) 150–156.
- [2] H. Rothe, C.A. Ryan, L. Page, J. Vinall, C. Goebel, H. Scheffler, F. Toner, C. Roper, P.S. Kern, Application of *in vitro* skin penetration measurements to confirm and refine the quantitative skin sensitization risk assessment of methylisothiazolinone, *Regul. Toxicol. Pharmacol.* 91 (2017) 197–207.
- [3] B. Desprez, M. Dent, D. Keller, M. Klaric, G. Ouédraogo, R. Cubberley, H. Duplan, J. Eilstein, C. Ellison, S. Grégoire, N.J. Hewitt, C. Jacques-Jamin, D. Lange, A. Roe, H. Rothe, B.J. Blauboer, A. Schepky, C. Mahony, A strategy for systemic toxicity assessment based on non-animal approaches: the cosmetics Europe long range science strategy programme, *Toxicol. in Vitro* 50 (2018) 137–146.
- [4] R.C. Wester, H.I. Maibach, Regional variation in percutaneous absorption: principles and application to human risk assessment, in: R.L. Bronaugh, H.I. Maibach (Eds.), *Percutaneous Absorption: Drugs-Cosmetics-Mechanisms-Methodology*, Fourth edition Marcel Dekker, Inc., New York 2005, pp. 85–93.
- [5] L. Duracher, L. Blasco, A. bdel Jaoued, L. Vian, G. Marti-Mestres, Irradiation of skin and contrasting effects on absorption of hydrophilic and lipophilic compounds, *Photochem. Photobiol.* 85 (2009) 1459–1467.
- [6] L.J. Mortensen, G. Oberdörster, A.P. Pentland, L.A. DeLouise, *In vivo* skin penetration of quantum dot nanoparticles in the murine model: the effect of UVR, *Nano Lett.* 8 (2008) 2779–2787.
- [7] C. Miquel-Jeanjean, F. Crépel, V. Raufast, B. Payre, L. Datas, S. Bessou-Touya, H. Duplan, Penetration study of formulated nanosized titanium dioxide in models of damaged and sun-irradiated skins, *Photochem. Photobiol.* 88 (2012) 1513–1521.
- [8] A. Chiang, E. Tudela, H.I. Maibach, Percutaneous absorption in diseased skin: an overview, *J. Appl. Toxicol.* 32 (2012) 537–563.
- [9] J.B. Nielsen, Percutaneous penetration through slightly damaged skin, *Arch. Dermatol. Res.* V296 (2005) 560–567.
- [10] S. Gattu, H.I. Maibach, Modest but increased penetration through damaged skin: an overview of the *in vivo* human model, *Skin Pharmacol. Physiol.* 24 (2011) 2–9.
- [11] OECD, OECD Guideline for the Testing of Chemicals, N° 428. Skin Absorption: *In vitro* Method, Paris, France, 2004 8.
- [12] SCCS, in: E.C. Consumers (Ed.), *Basic Criteria Forth In Vitro Assessment of Dermal Absorption of Cosmetic Ingredients* 2010, pp. 1–14.
- [13] K. Guth, M. Schäfer-Korting, E. Fabian, R. Landsiedel, B. van Ravenzwaay, Suitability of skin integrity tests for dermal absorption studies *in vitro*, *Toxicol. in Vitro* 29 (2015) 113–123.
- [14] F. Mohd, H. Todo, M. Yoshimoto, E. Yusuf, K. Sugibayashi, Contribution of the hair follicular pathway to total skin permeation of topically applied and exposed chemicals, *Pharmaceutics* 8 (2016).
- [15] S. Mitragotri, Y.G. Anissimov, A.L. Bunge, H.F. Frasch, R.H. Guy, J. Hadgraft, G.B. Kasting, M.E. Lane, M.S. Roberts, Mathematical models of skin permeability: an overview, *Int. J. Pharm.* 418 (2011) 115–129.
- [16] S. Mitragotri, Modeling skin permeability to hydrophilic and hydrophobic solutes based on four permeation pathways, *J. Control. Release* 86 (2003) 69–92.
- [17] D. Gerstel, C. Jacques-Jamin, A. Schepky, R. Cubberley, J. Eilstein, S. Grégoire, N. Hewitt, M. Klaric, H. Rothe, H. Duplan, Comparison of protocols for measuring cosmetic ingredient distribution in human and pig skin, *Toxicol. in Vitro* 34 (2016) 153–160.
- [18] A. Scott, F. Kalz, The penetration and distribution of C<sup>14</sup>-hydrocortisone in human skin after its topical application, *J. Investig. Dermatol.* 26 (1956) 149–158.
- [19] T. Rutherford, J.G. Black, The use of autoradiography to study the localization of germicides in skin, *Br. J. Dermatol.* 81 (1969) 75–87.
- [20] M. Suzuki, K. Asaba, H. Komatsu, M. Mochizuka, Autoradiographic study on percutaneous absorption of several oils useful for cosmetics, *J. Soc. Cosmet. Chem.* 29 (1978) 265–282.
- [21] E. Touitou, B. Fabin, S. Dany, S. Almog, Transdermal delivery of tetrahydrocannabinol, *Int. J. Pharm.* 43 (1988) 9–15.
- [22] H.J. Bidmon, J.D. Pitts, H.F. Solomon, J.V. Bondi, W.E.J.H. Stumpf, Estradiol distribution and penetration in rat skin after topical application, studied by high resolution autoradiography, *Histochemistry* 95 (1990) 43–54.
- [23] V. Raufast, A. Mavon, Transfollicular delivery of linoleic acid in human scalp skin: permeation study and microautoradiographic analysis, *Int. J. Cosmet. Sci.* 28 (2006) 117–123.
- [24] W.E. Stumpf, N. Hayakawa, H.-J. Bidmon, Skin research and drug localization with receptor microscopic autoradiography, *Exp. Dermatol.* 17 (2008) 133–138.
- [25] N. Hayakawa, N. Kubota, N. Imai, W.E. Stumpf, Receptor microscopic autoradiography for the study of percutaneous absorption, *in vivo* skin penetration, and cellular-intercellular deposition, *J. Pharmacol. Toxicol. Methods* 50 (2004) 131–137.
- [26] E.G. Solon, A. Schweitzer, M. Stoeckli, B. Prideaux, Autoradiography, MALDI-MS, and SIMS-MS imaging in pharmaceutical discovery and development, *AAPS J.* 12 (2010) 11–26.
- [27] C. Jacques, E. Perdu, E.L. Jamin, J.P. Cravedi, A. Mavon, H. Duplan, D. Zalko, Effect of skin metabolism on dermal delivery of testosterone: qualitative assessment using a new short-term skin model, *Skin Pharmacol. Physiol.* 27 (2014) 188–200.
- [28] C. Génies, E.L. Jamin, L. Debrauwer, D. Zalko, E.N. Person, J. Eilstein, S. Grégoire, A. Schepky, D. Lange, C. Ellison, A. Roe, S. Salhi, R. Cubberley, N.J. Hewitt, H. Rothe, M. Klaric, H. Duplan, C. Jacques-Jamin, Comparison of the metabolism of 10 chemicals in human and pig skin explants, *J. Appl. Toxicol.* 39 (2019) 385–397.
- [29] E.G. Solon, Autoradiography techniques and quantification of drug distribution, *Cell Tissue Res.* 360 (2015) 87–107.
- [30] M. Clench, J. Bunch, Imaging MALDI MS: an alternative to autoradiography for drug distribution studies? *Bio. Tech. Int.* 17 (2005) 20–23.
- [31] M. Stoeckli, D. Staab, A. Schweitzer, Compound and metabolite distribution measured by MALDI mass spectrometric imaging in whole-body tissue sections, *Int. J. Mass Spectrom.* 260 (2007) 195–202.
- [32] A.R. Buchberger, K. DeLaney, J. Johnson, L. Li, Mass spectrometry imaging: a review of emerging advancements and future insights, *Anal. Chem.* 90 (2018) 240–265.
- [33] K. Huber, T. Kunzke, A. Buck, R. Langer, B. Lubert, A. Feuchtinger, A. Walch, Multimodal analysis of formalin-fixed and paraffin-embedded tissue by MALDI imaging and fluorescence *in situ* hybridization for combined genetic and metabolic analysis, *Lab. Investig.* 99 (2019) 1535–1546.
- [34] J.M. Wiseman, D.R. Ifa, Q. Song, R.G. Cooks, Tissue imaging at atmospheric pressure using desorption electrospray ionization (DESI) mass spectrometry, *Angew. Chem. Int. Ed.* 45 (2006) 7188–7192.
- [35] P.C. Koopman, K.O. Nagornov, A.N. Kozhinov, D.P.A. Kilgour, Y.O. Tsybin, R.M.A. Heeren, S.R. Ellis, Increased throughput and ultra-high mass resolution in DESI FT-ICR MS imaging through new-generation external data acquisition system and advanced data processing approaches, *Sci. Rep.* 9 (2019) 1–11.
- [36] N.E. Manicke, A.L. Dill, D.R. Ifa, R.G. Cooks, High-resolution tissue imaging on an orbitrap mass spectrometer by desorption electrospray ionization mass spectrometry, *J. Mass Spectrom.* 45 (2010) 223–226.
- [37] M. Karas, D. Bachmann, U. Bahr, F. Hillenkamp, Matrix-assisted ultraviolet laser desorption of non-volatile compounds, *Int. J. Mass Spectrom. Ion Process.* 78 (1987) 53–68.
- [38] R.M. Caprioli, T.B. Farmer, J. Gile, Molecular imaging of biological samples: localization of peptides and proteins using MALDI-TOF MS, *Anal. Chem.* 69 (1997) 4751–4760.
- [39] J. Bunch, M.R. Clench, D.S. Richards, Determination of pharmaceutical compounds in skin by imaging matrix-assisted laser desorption/ionisation mass spectrometry, *Rapid Commun. Mass Spectrom.* 18 (2004) 3051–3060.
- [40] J.G. Swales, G. Hamm, M.R. Clench, R.J.A. Goodwin, Mass spectrometry imaging and its application in pharmaceutical research and development: a concise review, *Int. J. Mass Spectrom.* 437 (2019) 99–112.
- [41] M. Stoeckli, P. Chaurand, D.E. Hallahan, R.M. Caprioli, Imaging mass spectrometry: a new technology for the analysis of protein expression in mammalian tissues, *Nat. Med.* 7 (2001) 493–496.
- [42] B. Prideaux, S.J. Atkinson, V.A. Carolan, J. Morton, M.R. Clench, Sample preparation and data interpretation procedures for the examination of xenobiotic compounds in skin by indirect imaging MALDI-MS, *Int. J. Mass Spectrom.* 260 (2007) 243–251.
- [43] G. Loos, A.V. Schepdael, D. Cabooter, Quantitative mass spectrometry methods for pharmaceutical analysis, *Phil. Trans. R. Soc. A* 374 (2016), 20150366.

- [44] G. Hamm, D. Bonnel, R. Legouffe, F. Pamelard, J.-M. Delbos, F. Bouzom, J. Stauber, Quantitative mass spectrometry imaging of propranolol and olanzapine using tissue extinction calculation as normalization factor, *J. Proteome* 75 (2012) 4952–4961.
- [45] J.A. Barry, R. Ait-Belkacem, W.M. Hardesty, L. Benakli, C. Andonian, H. Licea-Perez, J. Stauber, S. Castellino, Multicenter validation study of quantitative imaging mass spectrometry, *Anal. Chem.* 91 (2019) 6266–6274.
- [46] L.M. Russell, R.H. Guy, Novel imaging method to quantify stratum corneum in dermatopharmacokinetic studies: proof-of-concept with acyclovir formulations, *Pharm. Res.* 29 (2012) 3362–3372.
- [47] G. Maddalo, F. Petrucci, M. Iezzi, T. Pannellini, P. Del Boccio, D. Ciavardelli, A. Biroccio, F. Forli, C. Di Ilio, E. Ballone, Analytical assessment of MALDI-TOF imaging mass Spectrometry on thin histological samples. An insight in proteome investigation, *Clin. Chim. Acta* 357 (2005) 210–218.
- [48] A.F.M. Altelaar, I.M. Taban, L.A. McDonnell, P.D.E.M. Verhaert, R.P.J. De Lange, R.A.H. Adan, W.J. Mooi, R.M.A. Heeren, S.R. Piersma, High-resolution MALDI imaging mass spectrometry allows localization of peptide distributions at cellular length scales in pituitary tissue sections, *Int. J. Mass Spectrom.* 260 (2007) 203–211.
- [49] P. Hart, S. Francese, E. Claude, N. Woodroffe, M. Clench, MALDI-MS imaging of lipids in ex vivo human skin, *Anal. Bioanal. Chem.* 401 (2011) 115–125.
- [50] M. Nishimura, M. Hayashi, Y. Mizutani, K. Takenaka, Y. Imamura, N. Chayahara, M. Toyoda, N. Kiyota, T. Mukohara, H. Aikawa, Y. Fujiwara, A. Hamada, H. Minami, Distribution of erlotinib in rash and normal skin in cancer patients receiving erlotinib visualized by matrix assisted laser desorption/ionization mass spectrometry imaging, *Oncotarget* 9 (2018) 18540–18547.
- [51] C.S. de Macedo, D.M. Anderson, K.L. Schey, MALDI (matrix assisted laser desorption ionization) imaging mass spectrometry (IMS) of skin: aspects of sample preparation, *Talanta* 174 (2017) 325–335.
- [52] D.W. Hunt, G.C. Winters, R.W. Brownsey, J.E. Kulpa, K.L. Gilliland, D.M. Thiboutot, H.E. Hofland, Inhibition of sebum production with the acetyl coenzyme a carboxylase inhibitor Olumacostat Glaseretil, *J. Investig. Dermatol.* 137 (2017) 1415–1423.
- [53] J. Lademann, H. Richter, M. Meinke, W. Sterry, A. Patzelt, Which skin model is the most appropriate for the investigation of topically applied substances into the hair follicles? *Skin Pharmacol. Physiol.* 23 (2010) 47–52.
- [54] N.A. Monteiro-Riviere, D.G. Bristol, T.O. Manning, R.A. Rogers, J.E. Riviere, Interspecies and interregional analysis of the comparative histologic thickness and laser Doppler blood flow measurements at five cutaneous sites in nine species, *J. Investig. Dermatol.* 95 (1990) 582–586.
- [55] J.P. Sandby-Møller, T. Poulsen, H.C. Wulf, Epidermal thickness at different body sites: relationship to age, gender, pigmentation, blood content, skin type and smoking habits, *Acta. Dermatol. Venereologica.* 83 (2003) 410–413.
- [56] E.A.W. Wolberink, P.E.J. van Erp, M.M. Teussink, P.C.M. van de Kerkhof, M.J.P. Gerritsen, Cellular features of psoriatic skin: Imaging and quantification using in vivo reflectance confocal microscopy, *80B* (2011) 141–149.
- [57] J.M. Spraggins, D.G. Rizzo, J.L. Moore, M.J. Noto, E.P. Skaar, R.M. Caprioli, Next-generation technologies for spatial proteomics: integrating ultra-high speed MALDI-TOF and high mass resolution MALDI FTICR imaging mass spectrometry for protein analysis, *Proteomics* 16 (2016) 1678–1689.
- [58] A. Smith, V. L'Imperio, V. Denti, M. Mazza, M. Ivanova, M. Stella, I. Piga, C. Chinello, E. Ajello, F. Pieruzzi, F. Pagni, F. Magni, High spatial resolution MALDI-MS imaging in the study of membranous nephropathy, *Proteomics Clin. Appl.* 13 (2019).
- [59] M.R. Groseclose, S. Castellino, Intramuscular and subcutaneous drug depot characterization of a long-acting cabotegravir nanof ormulation by MALDI IMS, *Int. J. Mass Spectrom.* 437 (2019) 92–98.
- [60] M. Niehaus, J. Soltwisch, M.E. Belov, K. Dreisewerd, Transmission-mode MALDI-2 mass spectrometry imaging of cells and tissues at subcellular resolution, *Nat. Methods* 16 (2019) 925–931.
- [61] A. Benninghoven, F.G. Rüdener, H.W. Werner, *Secondary Ion Mass Spectrometry—Basic Concepts, Instrumental Aspects, Applications and Trends*, Wiley, New York, 1987.
- [62] J.C. Vickerman, D. Briggs, *ToF-SIMS: Materials Analysis by Mass Spectrometry 2nd Edition*, Surface Spectra Limited, Manchester, 2013.
- [63] P. Van der Heide, *Secondary Ion Mass Spectrometry, An Introduction to Principles and Practices*, John Wiley & Sons, New York, 2014.
- [64] R.N.S. Sodhi, Time-of-flight secondary ion mass spectrometry (TOF-SIMS):—versatility in chemical and imaging surface analysis, *Analyst* 129 (2004) 483–487.
- [65] J.S. Fletcher, J.C. Vickerman, Secondary ion mass spectrometry: characterizing complex samples in two and three dimensions, *Anal. Chem.* 85 (2013) 610–639.
- [66] P. Sjövall, T.M. Greve, S.K. Clausen, K. Møller, S. Eirefelt, B. Johansson, K.T. Nielsen, Imaging of distribution of topically applied drug molecules in mouse skin by combination of time-of-flight secondary ion mass spectrometry and scanning electron microscopy, *Anal. Chem.* 86 (2014) 3443–3452.
- [67] G.S. Luengo, P. Halleot, F. Leroy, Nanoscale imaging and quantification of the impact of covalently linked lipids on the hair's surface, *Int. J. Cosmet. Sci.* 28 (2006) 147.
- [68] I.M. Kempson, W.M. Skinner, ToF-SIMS analysis of elemental distributions in human hair, *Sci. Total Environ.* 338 (2005) 213–227.
- [69] C. Bich, D. Touboul, A. Brunelle, Cluster ToF-Sims imaging as a tool for micrometric histology of lipids in tissue, *Mass Spectrom. Rev.* 33 (2014) 442–451.
- [70] C. Bich, R. Havelund, R. Moellers, D. Touboul, F. Kollmer, E. Niehuis, I.S. Gilmore, A. Brunelle, Argon cluster ion source evaluation on lipid standards and rat brain tissue samples, *Anal. Chem.* 85 (2013) 7745–7752.
- [71] P. Sjövall, L. Skedung, S. Gregoire, O. Biganska, F. Clément, G.S. Luengo, Imaging the distribution of skin lipids and topically applied compounds in human skin using mass spectrometry, *Sci. Rep.* 8 (2018), 16683.
- [72] M. Okamoto, K. Ishikawa, N. Tanji, S. Aoyagi, I. Kita, C.T. Migita, Structural analysis of the outermost hair surface using TOF-SIMS with C60 depth profiling technique, *e-J. Surf. Sci. Nanotechnol.* 10 (2012) 234–238.
- [73] N.J. Starr, K. Abdul Hamid, J. Wibawa, I. Marlow, M. Bell, L. Pérez-García, D.A. Barrett, D.J. Scurr, Enhanced vitamin C skin permeation from supramolecular hydrogels, illustrated using in situ ToF-SIMS 3D chemical profiling, *Int. J. Pharm.* 563 (2019) 21–29.
- [74] R. Castaing, G. Slodzian, Microanalyse par émission ionique secondaire (microanalysis by secondary ion emission), *J. Microsc.* 1 (1962) 395–410.
- [75] P. Galle, Tissue localization of stable and radioactive nuclides by secondary-ion microscopy, *J. Nucl. Med.* 23 (1982) 52–57.
- [76] P. Galle, J.P. Berry, F. Escaig, Secondary ion mass microanalysis: applications in biology, *Scan. Electron Microsc.* (1983) 827–839.
- [77] M.S. Burns, Applications of secondary ion mass spectrometry (SIMS) in biological research: a review, *J. Microsc.* 127 (1982) 237–258.
- [78] M.S. Burns, Biological microanalysis by secondary ion mass spectrometry: status and prospects, *Ultramicroscopy* 24 (1988) 269–281.
- [79] E. De Chambost, A history of Cameca (1954–2009), in: Peter W. Hawkes (Ed.), *Advances in Imaging and Electron Physics*, vol. 167, Elsevier 2011, pp. 1–119.
- [80] G. Slodzian, B. Daigne, F. Girard, F. Boust, F. Hillion, Scanning secondary ion analytical microscopy with parallel detection, *Biol. Cell.* 74 (1992) 43–50.
- [81] A. Benninghoven, W.K. Sichter mann, Detection, identification and structural investigation of biologically important compounds by secondary ion mass spectrometry, *Anal. Chem.* 50 (1978) 1180–1184.
- [82] S.R. Ellis, A.L. Bruinen, R.M. Heeren, A critical evaluation of the current state-of-the-art in quantitative imaging mass spectrometry, *Anal. Bioanal. Chem.* 406 (2014) 1275–1289.
- [83] M.S. Burns, D.M. File, Quantitative microlocalization of diffusible ions in normal and galactose cataractous rat lens by secondary ion mass spectrometry, *J. Microsc.* 144 (1986) 157–182.
- [84] J.-L. Guerquin-Kern, C. Borda, Cryo-preparation procedures for elemental imaging by SIMS and EFTEM, *Handbook of Cryo-Preparation Methods for Electron Microscopy*, CRC Press 2008, pp. 499–536.
- [85] P. Halléot, J.-N. Audinot, H.-N. Migeon, Direct NanoSIMS imaging of diffusible elements in surface block of cryo-processed biological samples, *Appl. Surf. Sci.* 252 (2006) 6706–6708.
- [86] R. Levi-Setti, G. Crow, Y.L. Wang, High-resolution topographic and isotopic imaging with a 40keV Ga<sup>+</sup> scanning ion microprobe, *Microbeam Anal.* (1985) 209–218.
- [87] R. Levi-Setti, Structural and microanalytical imaging of biological materials by scanning microscopy with heavy-ion probes, *Ann. Rev. Biophys. Chem.* 11 (1988) 325–347.
- [88] C. Lechene, F. Hillion, G. McMahon, D. Benson, A.M. Kleinfeld, J.P. Kampf, D. Distel, Y. Luyten, J. Bonventre, D. Hentschel, K.M. Park, S. Ito, M. Schwartz, G. Benichou, G. Slodzian, High-resolution quantitative imaging of mammalian and bacterial cells using stable isotope mass spectrometry, *J. Biol.* 5 (2006) 20.
- [89] J.L. Guerquin-Kern, T.D. Wu, C. Quintana, A. Croisy, Progress in analytical imaging of the cell by dynamic secondary ion mass spectrometry (SIMS microscopy), *Biochim. Biophys. Acta* 1724 (2005) 228–238.
- [90] J. Nuñez, R. Renslow, J.B. Cliff, C.R. Anderson, NanoSIMS for biological applications: current practices and analyses, *Biointerphases* 13 (2018), 03B301.
- [91] J.L. Guerquin-Kern, F. Hillion, J.C. Madelmont, P. Labarre, J. Papon, A. Croisy, Ultrastructural cell distribution of the melanoma marker iodobenzamide: improved potentiality of SIMS imaging in life sciences, *Biomed. Eng. Online* 3 (2004) 10.
- [92] P. Labarre, J. Papon, A.H. Rose, J.L. Guerquin-Kern, L. Morandeau, T.D. Wu, M.F. Moreau, M. Bayle, J.M. Chezal, A. Croisy, J.C. Madelmont, H. Turner, N. Moins, Melanoma affinity in mice and immunosuppressed sheep of [(125)I]N-(4-dipropylaminobutyl)-4-iodobenzamide, a new targeting agent, *Nucl. Med. Biol.* 35 (2008) 783–791.
- [93] M. Bonnet-Duquenois, J. Papon, F. Mishellany, P. Labarre, J.L. Guerquin-Kern, T.D. Wu, M. Gardette, J. Maublant, F. Penault-Llorca, E. Miot-Noirault, A. Cayre, J.C. Madelmont, J.M. Chezal, N. Moins, Targeted radionuclide therapy of melanoma: anti-tumoural efficacy studies of a new 131I labelled potential agent, *Int. J. Cancer* 125 (2009) 708–716.
- [94] N. Tanji, M. Okamoto, Y. Katayama, M. Hosokawa, N. Takahata, Y. Sano, Investigation of the cosmetic ingredient distribution in the stratum corneum using NanoSIMS imaging, *Appl. Surf. Sci.* 255 (2008) 1116–1118.
- [95] T. Wirtz, Imaging and analytics on the helium ion microscope, *Annu. Rev. Anal. Chem.* 12 (1) (2019).
- [96] B.M. Prentice, C.W. Chumbley, R.M. Caprioli, Absolute quantification of rifampicin by MALDI imaging mass spectrometry using multiple TOF/TOF events in a single laser shot, *J. Am. Soc. Mass Spectrom.* 28 (2017) 136–144.
- [97] C.W. Chumbley, M.L. Reyzer, J.L. Allen, G.A. Marriner, L.E. Via, C.E. Barry, R.M. Caprioli, Absolute quantitative MALDI imaging mass spectrometry: a case of rifampicin in liver tissues, *Anal. Chem.* 88 (2016) 2392–2398.
- [98] G.L. Long, J.D. Winefordner, Limit of detection. A closer look at the IUPAC definition, *Anal. Chem.* 55 (1983) 712A–724A.
- [99] P. Kolkhof, M. Delbeck, A. Kretschmer, W. Steinke, E. Hartmann, L. Bäracker, F. Eitner, B. Albrecht-Küpper, S. Schäfer, Finerenone, a novel selective nonsteroidal mineralocorticoid receptor antagonist protects from rat cardiorenal injury, *J. Cardiovasc. Pharmacol.* 64 (2014) 69–78.
- [100] S. Schulz, M. Becker, M.R. Groseclose, S. Schadt, C. Hopf, Advanced MALDI mass spectrometry imaging in pharmaceutical research and drug development, *Curr. Opin. Biotechnol.* 55 (2019) 51–59.
- [101] S. Giordano, L. Morosi, P. Veglianesi, S.A. Licandro, R. Frapolli, M. Zucchetti, G. Cappelletti, L. Falciola, V. Pifferi, S. Visentin, M. D'Incalci, E. Davoli, 3D mass spectrometry imaging reveals a very heterogeneous drug distribution in tumors, *Sci. Rep.* 6 (2016), 37027.
- [102] N.P. Lockyer, Secondary ion mass spectrometry imaging of biological cells and tissues, *Methods Mol. Biol.* (2014) 707–732.